Available online at www.sciencedirect.com
SCIENCE DIRECT
Thermochimica Acta 442 (2006) 42–47
thermochimica acta
www.elsevier.com/locate/tca

Evaluation of the reversible contribution to the reversing heat capacity in isotactic polystyrene

Hui Xu, Peggy Cebe *

Department of Physics and Astronomy, Tufts University, Medford, MA 02155, USA

Available online 20 December 2005

Abstract

We report the results of time dependent analysis of the reversing heat capacity peaks in isotactic polystyrene (iPS). Solution grown crystals (SGCs) and bulk films of iPS were examined using quasi-isothermal temperature modulated differential scanning calorimetry (QI-TMDSC). Both types of iPS samples showed two reversing heat capacity peaks as reported before [H. Xu, P. Cebe, Macromolecules 37 (2004) 2797; H. Xu, P. Cebe, Macromolecules 38 (2005) 770], and the two peaks are associated with melting of different portions of crystal lamellae with different degree of thermal stability [T. Liu, J. Petermann, Polymer 42 (2001) 6453]. Here, the behavior of the reversing heat capacity is studied as a function of holding time from the establishment of steady state, until the end of the quasi-isothermal holding period. The reversing heat capacity decreases with time at each of the two peak positions. For both types of iPS (SGC and bulk film) the time dependence of each of the reversing heat capacity peaks is fitted using $C_p(t) = C_{p\infty} + A_1 \exp(-t/\tau_1) + A_2 \exp(-t/\tau_2)$. The fit parameters (equilibrium reversible heat capacity, $C_{p\infty}$; prefactors, A_1 and A_2; relaxation times, τ_1 and τ_2) provide a means to compare the decay of the dual reversing heat capacity peaks of iPS solution grown crystals with bulk cold-crystallized film. Results show that iPS bulk films have longer relaxation times (τ_1 and τ_2) and smaller $C_{p\infty}$ value than the iPS SGCs. Both results suggest that the iPS bulk films have higher degree of crystal perfection than SGCs.

Keywords: Reversing heat capacity; Isotactic polystyrene; Differential scanning calorimetry

1. Introduction

Quasi-isothermal temperature modulated differential scanning calorimetry (QI-TMDSC) has been used to characterize the reversing melting of semicrystalline polymers [1,2,4–10]. Using this technique a small locally reversible melting has been found in several flexible linear macromolecules, including iPS [1,2,4–10]. The concept of molecular nucleation was first introduced by Wunderlich and co-workers [5,10,11] and has been used to explain the reversible latent heat contribution in the melting range. Molecular nucleation is a process that requires a flexible polymer chain to go through a nucleation step before adding to the growth surface of the crystal [11]. The amount of the reversible melting is typically quite small, and is considered to be a local process that occurs on a molecular length scale at the interface between the crystal and the surrounding melt [4–10].

To review briefly, the QI-TMDSC technique, developed by Wunderlich and co-workers, and others [4–10,12,13] involves setting the underlying temperature at T_0 while applying a small amplitude sinusoidal oscillation about T_0. This condition is held for some period of time, and then the temperature T_0 is increased to a new value. After steady state is achieved at T_0 (as judged by the appearance of the Lissajous figure of modulated heat flow versus modulated temperature [1,14]) the reversing heat capacity is measured as a function of holding time at T_0. Details about the QI-TMDSC technique can be found in other references [15,16], and in the interests of brevity they will not be repeated here. The reversing heat capacity measured in QI-TMDSC is considered an "apparent" heat capacity since the contributions of latent heat are included in $C_p(t)$ [6,17,18].

Using QI-TMDSC, we recently reported on two types of semicrystalline iPS, which varied in their preparation history. IPS bulk film was cold crystallized by heating from the glassy state [1] and iPS solution grown crystals (SGCs) were prepared from dilute solution [2]. The iPS bulk films had smaller degrees of crystallinity, and greater amounts of the rigid amorphous fraction, compared to the SGCs, which were prepared under conditions of increased molecular mobility. In spite of these differences, both SGCs and bulk films of iPS exhibited multiple melting endotherms in standard DSC scanning, and

* Corresponding author. Tel.: +1 617 6273365; fax: +1 617 6273744.
E-mail address: peggy.cebe@tufts.edu (P. Cebe).

0040-6031/$ – see front matter © 2005 Elsevier B.V. All rights reserved.
doi:10.1016/j.tca.2005.11.015

dual reversing melting in QI-TMDSC experiments [1,2]. First, observation of reversing melting of iPS supports the mechanism of polymer reversing melting proposed by Wunderlich and co-workers [4–11]. Second, observation of dual reversing melting supports the proposal of Liu and Petermann [3], based on transmission electron microscopic studies, that iPS has different thermal stability distributions, along a single lamella, leading to multiple melting in this polymer. Here, we investigate the stability of the reversing melting peaks, by evaluating the time dependence of the reversing heat capacity, $C_p(t)$, at selected temperatures during the QI-TMDSC measurement.

It has been shown that the reversing melting peak height decreases with time and with crystal perfection [9,10,19]. According to Pyda et al. [9,10] and Schick et al. [19], the decrease of reversing heat capacity with time is not caused by the temperature modulation in TMDSC, but is due to recrystallization and annealing. The study of time dependent reversing heat capacity allows us to separate the locally reversible process from the irreversible events, e.g. recrystallization, annealing, and evaluate the equilibrium reversible heat capacity, $C_{p\infty}$, which is the value of the heat capacity in the limit of infinite holding time at T_0 when all the irreversible process is finished. Practically, the assessment of $C_{p\infty}$ is made by modeling the decrease of $C_p(t)$ for finite times, and using the model parameters to infer the infinite-time value [9,10,19]. According to Wunderlich, the equilibrium reversible heat capacity is the key to estimating the truly reversible melting and crystallization [20,21]. In this work, following the method of Schick et al. [19] and Pyda et al. [9,10], we use two exponential functions to evaluate the equilibrium reversible heat capacity in the melting range of the iPS cold-crystallized bulk film, and iPS solution grown crystals.

To evaluate the reversibility of melting or crystallization, the following conditions should be met [22–24]. Either, (1) we must be able to monitor the change of total heat capacity while measuring the equilibrium reversible heat capacity [22–24], or (2) we must be able to evaluate the thermodynamic vibrational heat capacity, obtained from the global phase fractions by extending the time to infinity after the irreversible process is finished.

In practice, however, it is not possible to achieve these conditions. The *simultaneous* measurement of total heat capacity and equilibrium reversible heat capacity is not possible, since the latter is measured under conditions of heating rate equal to zero. And, polymer molecules nearly always experience extensive reorganization, and annealing processes during equilibrium reversible heat capacity measurements, especially within the major crystallization or melting region. Thus, the evaluation of the thermodynamic vibrational heat capacity is difficult [22,23]. However, for some polymer systems, by varying the experimental parameters, it is possible to evaluate the thermodynamic vibrational heat capacity and equilibrium reversible heat capacity in separate experiments, and obtain the reversibility of melting, provided the reversible transition is far away from major melting and crystallization events [22,23].

In crystallized iPS, below the temperatures of melting region, both total heat capacity and reversing heat capacity show no excess enthalpy production, and the global structure is stable. Within the melting region, the iPS molecules undergo a strong annealing, recrystallization, or reorganization process. Thus, it seems not possible either to obtain the thermodynamic vibrational heat capacity, or to measure simultaneously the total heat capacity and equilibrium reversible heat capacity. Therefore, in this work, our focus is to evaluate the equilibrium reversible heat capacity in the melting range of the cold-crystallized iPS and iPS solution grown crystals using the data taken under quasi-isothermal TMDSC conditions.

We find that iPS SGCs have relatively stronger reversible melting than bulk iPS. For the bulk iPS, the upper peak of the equilibrium reversible heat capacity is just slightly greater than the iPS liquid heat capacity indicating the bulk material has weaker reversible melting. At the same time, the irreversible processes, of annealing and recrystallization during long time holding at constant temperature, are characterized by the fitting model. By comparing the fitting parameters, we find that iPS bulk films have greater relaxation times both in the process of annealing and recrystallization, than the iPS SGCs. The recrystallization is relatively stronger in the iPS bulk film due to its initially smaller crystalline content. All the results confirm that iPS bulk film is in the more perfect and stable form than its SGC counterpart.

2. Experimental

Isotactic (90%) polystyrene powder with a weight-average molecular weight of 400,000 g/mol was obtained from Scientific Polymer Products, Inc. The powder of iPS was compression molded at 523 K for 3 min, then quenched into cold water to obtain the amorphous bulk films. The amorphous samples were isothermally cold crystallized in a Mettler FP90 hot stage by heating them to 443 K and holding for 4 h until crystallization was complete. A self-seeding technique was applied to grow iPS crystals in DMP dilute solution [25]. The detailed description of iPS SGC preparation is given in reference [2]. The solution concentration was 0.05 wt% and crystallization temperature was 373 K and holding time was 2 weeks. After the crystallization, the solution with precipitated crystals was slowly filtered at room temperature under slight suction to form a mat. The crystal mats were rinsed and washed with methanol several times to remove residual DMP. Finally, the SGC sample was dried in a vacuum oven for 24 h at room temperature. The crystallinity was determined from FTIR analysis and wide angle X-ray diffraction [26], and endotherm analysis [1,2]. The cold-crystallized bulk iPS had crystalline fraction 0.40 whereas the SGC iPS had crystalline fraction of 0.49.

The reversing heat capacity was measured under quasi-isothermal conditions using a TA Instruments DSC 2920 under modulated mode. The temperature was calibrated using indium in the standard DSC mode with heating rate at 10 K/min. The quasi-isothermal TMDSC experiment was carried out at temperature, T_0, over the temperature range of 420–520 K with a stepwise temperature increase of 2 K or 2.5 K. The temperature modulation amplitude is 0.5 K, and oscillation period is 1 min. Each quasi-isothermal run lasted 100 min, and the reversing heat capacity at given T_0 was analyzed only for times after the first five cycles. Three runs containing baseline, sapphire standard

and sample have been executed to obtain the reversing heat capacity of the sample. Detailed information for obtaining the reversing heat capacity is given in references [1,2].

The appearance of the Lissajous figure was used to verify that the steady state was achieved [1,2]. The steady state in this study refers to the condition that the modulated heat flow and the modulated temperature have the same oscillation frequency, and the phase lag is constant, so that the calculation of reversing heat capacity using first harmonic of the Fourier transform of the modulated heat flow and modulated temperature is valid. The establishment of the steady state can be verified by the appearance of the perfect ellipse when plotting modulated heat flow vs. modulated temperature.

3. Results and discussion

Fig. 1 shows the reversing heat capacity (open circles) for cold-crystallized iPS [1] obtained from quasi-isothermal TMDSC experiments with isothermal holding time of 20 min per step. In Fig. 1, the dotted line is the heat capacity of liquid iPS, and the dashed line is the heat capacity of solid iPS both of which are obtained from the ATHAS data bank [27]. Our own measured liquid and solid heat capacities matched the values from the ATHAS data bank very well as was shown in reference [1]. Two tiny reversing heat capacity maxima are located in Fig. 1 by vertical lines at $T_{m1} = 477$ K and $T_{m2} = 502$ K. These lines mark the greatest values of the reversing heat capacity in the QI-TMDSC experiment after 20 min holding time per step (open circles). The solid symbols represent the values of the equilibrium reversible heat capacity of cold-crystallized iPS determined by modeling, which will be discussed later on.

Fig. 2 shows the reversing heat capacity (open circles) for iPS SGCs, crystallized for 2 weeks at 373 K [2] obtained from quasi-isothermal TMDSC experiments with isothermal holding time of 20 min per step. The two reversing heat capacity maxima are much stronger in the SGC iPS (Fig. 2) than in the cold-crystallized iPS (Fig. 1). Their peak positions are marked with vertical lines at $T_{m1} = 474$ K and $T_{m2} = 500$ K. The liquid (dotted line) and solid (dashed line) heat capacities from the ATHAS data bank [27] are also shown. The solid symbols in Fig. 2 represent the values of the equilibrium reversible heat capacity of SGCs of iPS, determined by modeling, which will be discussed later on.

For comparison, we also show in Figs. 1 and 2, the computed sigmoidal baseline heat capacity (solid curve, right hand vertical

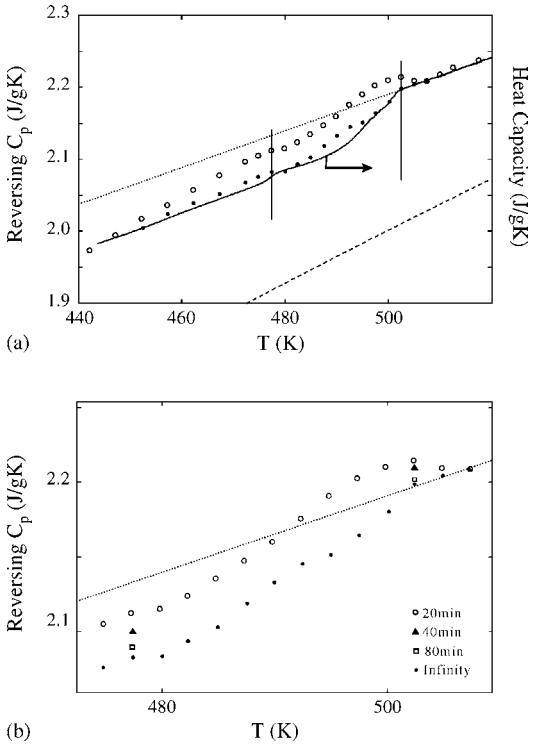

Fig. 1. Reversing heat capacity traces measured in QI-TMDSC measurements (open circles) and the corresponding equilibrium reversible heat capacity, $C_{p\infty}$ (solid circles) obtained by fitting from Eq. (1), for iPS cold crystallized at $T_c = 443$ K, $t_c = 4$ h [1]. The dotted line is the heat capacity of liquid iPS, and dashed line is the heat capacity of solid iPS, both obtained from the ATHAS data bank [27]. (a) Wide scaling. The solid line, referring to the right hand vertical axis, is the computed sigmoidal baseline heat capacity within the melting region acquired from a standard DSC scan [1,2], for comparison purposes. (b) Expanded scaling. The points with maximum values of heat capacity near the peak positions are marked with vertical solid lines in (a).

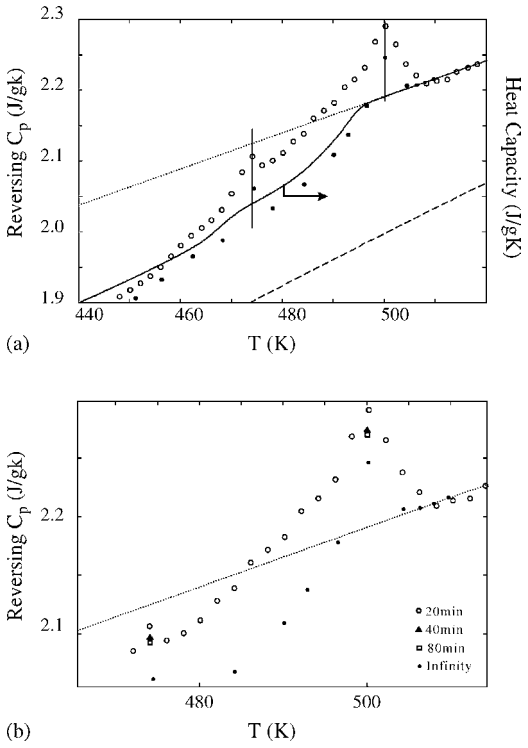

Fig. 2. Reversing heat capacity traces measured in QI-TMDSC measurements (open circles) and the corresponding equilibrium reversible heat capacity, $C_{p\infty}$ (solid circles) obtained by fitting from Eq. (1), for iPS SGC crystallized at $T_c = 373$ K, $t_c = 2$ weeks [2]. The dotted line is the heat capacity of liquid iPS, and dashed line is the heat capacity of solid iPS, both obtained from the ATHAS data bank [27]. (a) Wide scaling. The solid line, referring to the right hand vertical axis, is the computed sigmoidal baseline heat capacity within the melting region acquired from a standard DSC scan [1,2], for comparison purposes. (b) Expanded scaling. The points with maximum values of heat capacity near the peak positions are marked with vertical solid lines in (a).

axis) within the melting region acquired from a standard DSC scan at a heating rate of 10 K/min [1,2]. From the standard DSC scan, the temperature dependence of the crystalline fraction was assessed using Euler's method [1,2]. The computed sigmoidal baseline (solid curve) represents the underlying reversing heat capacity within the melting region, for the standard DSC scan, and is shown for comparative purposes. One should be aware that the computed sigmoidal baseline heat capacity is heating rate dependent. Thus, the baseline shown in Figs. 1a and 2a cannot serve as a baseline heat capacity for the zero heating rate measurements of the reversing heat capacity. However, the comparison between this computed sigmoidal baseline heat capacity from standard DSC, and the reversing heat capacity traces (open circles) demonstrates the annealing effects that occur during the extremely slow heating used in the quasi-isothermal TMDSC experiments.

For example, in the cold-crystallized iPS (Fig. 1a) the computed sigmoidal baseline heat capacity (solid curve) reaches the liquid heat capacity curve (dotted line) at the temperature indicated by the vertical line. But the reversing heat capacity (open circles) does not reach the liquid heat capacity curve until a temperature higher than that indicated by the vertical line. The annealing effect is even more apparent in the SGC iPS (Fig. 2a). The computed sigmoidal baseline heat capacity (solid curve) reaches the liquid heat capacity curve (dotted line) at 498 K, whereas the reversing heat capacity (open circles) reaches the liquid heat capacity (within experimental error) at about 507 K. This comparison shows that iPS crystals melt completely at lower temperature during standard DSC scanning. During the very slow heating conditions of QI-TMDSC, the iPS crystals become annealed so that they melt completely at higher temperatures. These results are consistent with the rapid heating rate studies by Schick and co-workers [28,29]. Besides the effect of annealing seen in Fig. 2a, we can also observe further crystallization in the QI-TMDSC scan for the SGC iPS. This is reflected by the negative deviation of the equilibrium reversible heat capacity from the standard baseline, since this SGC sample has lower crystalline content compared to samples crystallized at the other temperatures [2].

From Figs. 1a and 2a, we notice that the melting temperatures (indicated by the vertical lines) of cold-crystallized iPS (Fig. 1a) are higher than their SGC counterpart (Fig. 2a). The crystals annealed during the QI-TMDSC measurement are more perfected in originally cold-crystallized bulk iPS, and consequently melt at higher temperature. The reversing heat capacity amplitude may be assessed from the peak height over and above the liquid heat capacity curve. From this comparison, we find that the reversing melting heat capacity is larger for the iPS SGC sample. Such a result confirms that the amount of reversing melting decreases with crystal perfection [19]. Poorer crystal leads to higher degree of reversing melting in TMDSC.

An important issue demonstrated in earlier work by Okazaki and Wunderlich [5], Schick et al. [19], and Pyda et al. [9] is that the reversing heat capacity decreases with holding time. Following these works, in this study, we fit the time dependent reversing heat capacity, $C_p(t)$, with the sum of two exponential functions of the form:

$$C_p(t) = A_1 \exp\left(-\frac{t}{\tau_1}\right) + A_2 \exp\left(-\frac{t}{\tau_2}\right) + C_{p\infty} \quad (1)$$

where $C_{p\infty}$ is the equilibrium reversible heat capacity, A_1 and A_2 the prefactors, and τ_1 and τ_2 are the decay times (relaxation time). According to Pyda et al. [9], each exponential function represents an irreversible process: the first term, with shorter relaxation time τ_1, describes the recrystallization process, and the second term, with longer relaxation time τ_2, describes the annealing/perfection process. As time approaches infinity, all the irreversible events, including recrystallization and annealing, are finished. The only term remaining in the $C_p(t)$ is the truly reversible component $C_{p\infty}$. Thus, extrapolation to $t = \infty$ allows us to evaluate the equilibrium reversible component of the total melting [9,10,19].

Fig. 3 shows examples of the fits to the measured reversing heat capacity at constant temperature, using Eq. (1). The temperatures are those indicated by the vertical lines in Figs. 1a and 2a, reflecting the locations of the peak values of the reversing heat capacity traces. In Fig. 3, the data points (open circles) are the experimental data, and solid curves are fitted sum of two exponential functions of Eq. (1). Fig. 3a and b is for the bulk iPS at $T_{m1} = 477$ K and $T_{m2} = 502$ K, respectively. Fig. 3c and d is for the iPS SGCs at $T_{m1} = 474$ K and $T_{m2} = 500$ K, respectively. The parameters of best fit are listed in Table 1.

Eq. (1) was applied to the entire data set, for temperatures in the range where the dual reversing melting peaks were observed. We obtain the equilibrium reversible heat capacity, $C_{p\infty}$, over the whole temperature range based on the measured reversing heat capacity. In Figs. 1a and 2a, the data points represented by dark solid circles are the $C_{p\infty}$ obtained by fitting the measured reversing heat capacity at each temperature using Eq. (1). Figs. 1b and 2b are the expanded views of 1a and 2a, respectively, giving the time evolution of the reversing heat capacity at two selected peak positions (viz., T_{m1} and T_{m2}). In Figs. 1b and 2b, the open circle is for the reversing heat capacity at time of 20 min, the solid triangle is at time of 40 min, the open square is at time of 80 min, and the solid circle is at $t = \infty$.

Since we are neither able to evaluate the global phase structures at each temperature within the melting region when extending the time to infinity (due to intensive annealing), nor able to measure the total heat capacity simultaneously,

Table 1
Fitting parameters[a] for iPS at the peak positions of reversing melting

Sample	Bulk film[b]		Solution grown crystals[c]	
	Lower peak	Upper peak	Lower peak	Upper peak
Temperature (K)	477	502	474	500
A_1 (J/g K)	0.21	0.43	0.08	0.20
A_2 (J/g K)	0.03	0.05	0.02	0.02
τ_1 (min)	3.0	3.2	2.2	2.4
τ_2 (min)	35.0	33.1	33.4	32.0
$C_{p\infty}$ (J/g K)	2.07	2.19	2.06	2.22

[a] Fits are shown by the solid curves in Fig. 3, obtained using Eq. (1).
[b] iPS bulk film cold crystallized at 443 K for 4 h.
[c] iPS solution grown crystals, grown in DMP at 373 K for 2 weeks.

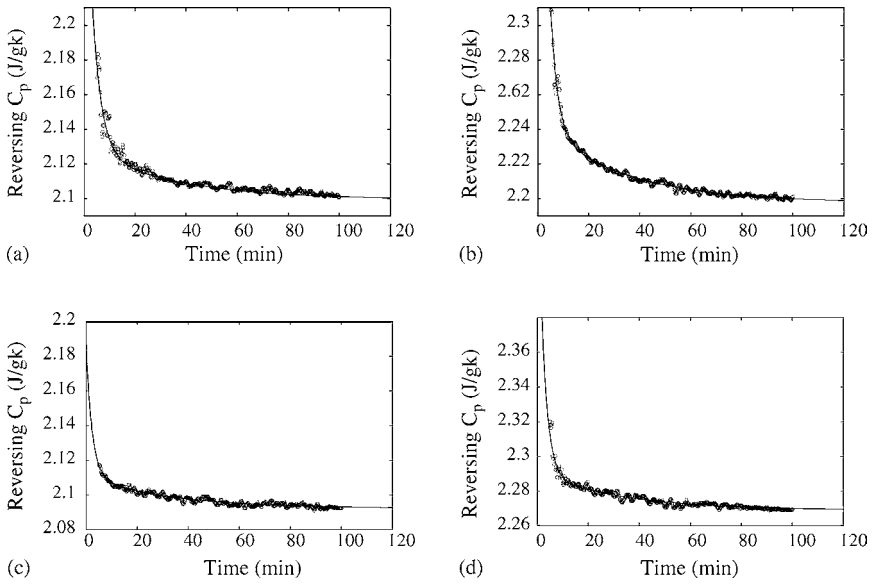

Fig. 3. Examples of fits (solid lines) to the measured reversing heat capacity data (open circles), at constant temperature, using Eq. (1) and the fitting parameters listed in Table 1. The abscissa is the holding time during the quasi-isothermal TMDSC measurement. The temperatures are chosen as the positions of the two vertical lines in Figs. 1a and 2a. (a) Cold-crystallized iPS bulk film, at T_{m1} = 477 K; (b) cold-crystallized iPS bulk film at T_{m2} = 502 K; (c) iPS SGC at T_{m1} = 474 K; (d) iPS SGC at T_{m2} = 500 K.

the thermodynamic baseline heat capacity for the equilibrium reversible heat capacity is not accessible. Thus, it is very hard to specify the true latent heat involved in the locally reversible melting process. A quantitative description of the specific reversibility of melting cannot be made. The material could experience strong annealing (increased crystal perfection) during the quasi-isothermal TMDSC experiments, which would result in an increase of the melting temperature. We suspect that the curve of the true thermodynamic baseline for the equilibrium reversing heat capacity probably will shift to higher temperature compared to the computed sigmoidal baseline heat capacity from standard DSC (solid curve) shown in Figs. 1a and 2a. The specific shape of the thermodynamic baseline remains unknown, so we cannot predict the appearance of the lowest peak (T_{m1}) of reversing heat capacity due to intensive annealing. It could remain at the same temperature location or, more probably, become shifted to higher temperature.

For the upper peak of the reversing heat capacity (T_{m2}), we need to distinguish the behavior of the iPS SGCs from the iPS bulk film. For iPS SGCs, Fig. 2a shows that the equilibrium reversible heat capacity (solid circles) is well above the liquid heat capacity (dotted line). This observation suggests that, after the irreversible process is finished, the system globally reaches equilibrium and a local reversible melting occurs at the remaining crystal surface under temperature modulation [20–23]. However, for the iPS bulk film, the situation is more complicated. In Fig. 1a, the value of the equilibrium reversible heat capacity at T_{m2} is just slightly over the heat capacity of the liquid, and we cannot determine unequivocally whether it still remains as a peak or not. By considering the possible shift of the baseline to higher temperature, we would expect that the equilibrium reversible heat capacity at T_{m2} for the bulk film might probably still be above the thermodynamic baseline, which means a reversible melting involving latent heat could still occur. Comparing Fig. 1a and Fig. 2a at the upper peak (T_{m2}), it is apparent that the total amount of reversible melting of iPS SGCs is relatively higher than that of bulk iPS, but the comparison of the specific reversibility of melting cannot be determined because of the lack of the thermodynamic baseline heat capacity.

IPS is one of the first polymers to show dual reversing melting endotherms [1,2]. By fitting the decay of the $C_p(t)$ using Eq. (1), we can compare the time dependence of each of the two reversing melting peaks. For the same sample, the relaxation time τ_2, describing the annealing, is longer for the lower temperature peak than for the higher temperature peak. This is most likely associated with the fact that annealing of iPS occurs more quickly at higher temperatures, as has been demonstrated in other polymer systems [7,8,11,19]. On the other hand, the relaxation time τ_1, describing the recrystallization, is longer for the higher temperature peak than for the lower temperature peak. The word "recrystallization" as applied here refers to a complex process involving continuous melting and recrystallization [9]. At the higher temperature peak, the overall process is more favorable to the melting since the temperature is much closer to the final melting point. Thus, at these high temperatures, the vitrification (due to recrystallization) is hindered, and consequently is slowed down. Therefore, τ_2(lower peak) > τ_2(upper peak) while τ_1(lower peak) < τ_1(upper peak) leads us to conclude that the lower peak anneals more slowly than the upper peak, while the upper peak recrystallizes more slowly than the lower peak. More importantly, for both lower and upper peaks of the dual reversing melting, the relaxation characterizing the annealing process is much slower than the relaxation characterizing the recrystallization process, i.e., $\tau_2 > \tau_1$.

Furthermore, we are able to compare two different types of iPS: cold-crystallized bulk film and solution grown crystals. Prior work [1,2] used standard DSC to show that SGCs, while possessing greater degree of crystallinity than bulk iPS, had

much broader endotherms and lower endotherm peak temperatures. These facts suggest that the SGCs are in fact comprised of less perfect crystals than the cold-crystallized bulk film. Comparing the decay of the reversing melting of the two iPS materials, we find that both relaxation times (τ_2 and τ_1) of the cold-crystallized bulk iPS are longer than those of the SGCs, when compared at roughly similar temperatures. This observation confirms that the iPS bulk film is more perfect than the iPS SGCs, and is more stable against annealing. The solution grown crystals anneal faster (smaller τ_2) and recrystallize faster (smaller τ_1).

From Eq. (1), we consider the difference, $C_{p\infty} - C_p(t=0) = A_1 + A_2$. The meaning of $C_{p\infty}$ is the truly reversible part of the heat capacity, which remains at infinite time. $A_1 + A_2$ reflects the sum of the two irreversible processes that cause $C_p(t)$ to decay. From Table 1 we see that the prefactor, A_1, representing the recrystallization, is always the larger contribution to the irreversible processes of both upper (90% for bulk iPS; 91% for SGC iPS) and lower peaks (88% for bulk iPS; 80% for SGC iPS). Recrystallization dominates the irreversible processes in both bulk and SGC iPS. The annealing process makes a much smaller contribution at both the upper and lower peak positions. The annealing contribution is largest in SGC iPS at the lower peak position, where is makes up 20% of the irreversible processes.

Finally, from Figs. 1b and 2b, we observe clear differences between the iPS bulk film and iPS SGCs. The bulk film decays to a value $C_{p\infty}$ (bulk) at the upper peak position, which is barely above the extrapolated heat capacity of liquid iPS. The SGC, on the other hand, maintains a clear and strong peak in $C_{p\infty}$ at both the lower and upper peak positions. The existence of the peaks at infinite time confirms that the SGCs contain less perfect crystals that continue to exhibit reversibility of melting.

4. Conclusion

By fitting our reversing melting heat capacity data with the sum of two exponential functions, we study the equilibrium reversible heat capacity contribution to the total melting. We investigate not only the decay of both of the dual reversing melting peaks, but also we compare two different semicrystalline iPS materials. IPS bulk film, cold crystallized from the glassy state, and iPS crystallized from dilute solution have very different relaxation behaviors. Since practically we are unable to determine the thermodynamic baseline heat capacity due to intensive annealing at slow heating for infinite holding time, the true latent heat contribution from the reversible melting is not obtained. However, we found that the total amount of reversible melting at upper melting peak for the iPS SGC is stronger than the bulk. By comparing the fitting parameters obtained using the formula, at similar temperatures, the iPS bulk films have longer annealing relaxation times in the irreversible process of annealing and recrystallization than the iPS solution grown crystals. All the evidence draws the conclusion that the iPS bulk film is in a more stable form than SGCs.

Acknowledgments

The authors thank the National Science Foundation, Polymers Program of the Division of Materials Research for support of this research through DMR-0100646.

References

[1] H. Xu, P. Cebe, Macromolecules 37 (2004) 2797.
[2] H. Xu, P. Cebe, Macromolecules 38 (2005) 770.
[3] T. Liu, J. Petermann, Polymer 42 (2001) 6453.
[4] M. Di Lorenzo, M. Pyda, B. Wunderlich, J. Polym. Sci. Part B: Polym. Phys. 39 (2001) 1594.
[5] I. Okazaki, B. Wunderlich, Macromol. Chem. Rapid Commun. 18 (1997) 313.
[6] K. Ishikiriyama, B. Wunderlich, Macromolecules 30 (1997) 4126.
[7] A. Wurm, C. Schick, Colloid. Polym. Sci. 281 (2003) 113.
[8] M. Pyda, B. Wunderlich, J. Polym. Sci. Part B: Polym. Phys. 38 (2000) 622.
[9] M. Pyda, M. Di Lorenzo, J. Pak, P. Kamasa, A. Buzin, J. Grebowicz, B. Wunderlich, J. Polym. Sci. Part B: Polym. Phys. 39 (2001) 1565.
[10] M. Di Lorenzo, M. Pyda, B. Wunderlich, J. Polym. Sci. Part B: Polym. Phys. 39 (2001) 1594.
[11] B. Wunderlich, Prog. Polym. Sci. 28 (2003) 383.
[12] A. Toda, C. Tomita, M. Hikosaka, J. Thermal Anal. Calorim. 54 (1998) 623.
[13] A. Toda, C. Tomita, M. Hikosaka, Y. Saruyama, Thermochim. Acta 324 (1998) 95.
[14] B. Wunderlich, A. Boller, I. Okazaki, S. Kreitmeier, Thermochim. Acta 282 (1996) 143.
[15] A. Boller, Y. Jin, B. Wunderlich, J. Thermal Anal. 42 (1994) 307.
[16] A. Boller, I. Okazaki, K. Ishikiriyama, G. Zhang, B. Wunderlich, J. Thermal Anal. 49 (1997) 1081.
[17] K. Ishikiriyama, B. Wunderlich, J. Polym. Sci. Part B: Polym. Phys. 35 (1997) 1877.
[18] B. Wunderlich, Thermochim. Acta 300 (1997) 43.
[19] C. Schick, M. Merzlyakov, B. Wunderlich, Polym. Bull. 40 (1998) 297.
[20] R. Androsch, B. Wunderlich, Macromolecules 34 (2001) 5950.
[21] R. Androsch, B. Wunderlich, Thermochim. Acta 369 (2001) 67.
[22] R. Androsch, B. Wunderlich, J. Polym. Sci. Part B: Polym. Phys. 41 (2003) 2039.
[23] R. Androsch, B. Wunderlich, J. Polym. Sci. Part B: Polym. Phys. 41 (2003) 2157.
[24] J. Pak, B. Wunderlich, J. Polym. Sci. Part B: Polym. Phys. 40 (2002) 2219.
[25] H.D. Keith, R.G. Vadimsky, F.J. Padden, J. Polym. Sci. Part B: Polym. Phys. 8 (1970) 1687.
[26] H. Xu, B.S. Ince, P. Cebe, J. Polym. Sci. Part B: Polym. Phys. 41 (2003) 3026.
[27] M. Pyda (Ed.), ATHAS data bank, http://web.utk.edu/~athas/databank/, 1994.
[28] A.A. Minakov, D.A. Mordvintsev, C. Schick, Polymer 45 (2004) 3755.
[29] S.A. Adamovsky, A.A. Minakov, C. Schick, Thermochim. Acta 403 (2003) 55.